Table I. Values of the Energy Differences Δ between the Minima and of the Energy Differences between the Gerade–Ungerade States in au[a]

	ref	Δ	δ	ρ	P_B(max)
methyloxonium ion	2	4.054×10^{-4}	1.626×10^{-5}	24.0	0.0017
α-methyl-β-hydroxyacrolein	5	8.400×10^{-4}	9.257×10^{-5}	9.130	0.0110
2-methylnaphthazarin	4	1.430×10^{-3}	1.530×10^{-9}	930000.0	0.0000
9-hydroxyphenalen-1-one	9	7.355×10^{-4}	4.810×10^{-4}	1.529	0.3000

[a] We also list values of the asymmetry parameter ρ and of P_B(max) for various molecules.

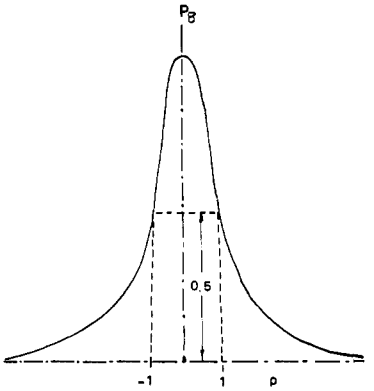

Figure 2. Plot of the probability P_B of finding the proton at time $t = \pi/2\omega$ as a function of the asymmetry parameter $\rho = \Delta/2\delta$. The half-width of the Lorentzian curve corresponds to $\rho = 1$.

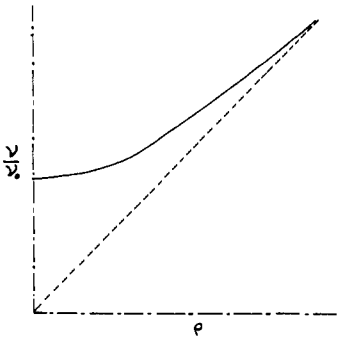

Figure 3. Ratio of the frequencies ν and ν_0 as a function of the asymmetric parameter ρ. The frequency ν increases with the asymmetry of the double-minimum potential.

Discussion

The coefficients P_A and P_B of eq 13 represent the probabilities of finding the proton either in well A or in well B, respectively. At time $t = 0$, the particle is in well A. The maximum probability of finding the particle in well B is

$$q = P_B(\max) = \cos^2 \alpha = 1/(1 + \rho^2) \qquad (14)$$

and it occurs when $\omega t = (n + {}^1/_2)\pi$.

Equation 13 presents a clear and simple description of the effect of the perturbation on tunnelling. It is easily seen that only the fraction q defined by eq 14 will tunnel. The fraction q is a Lorentzian with half-width equal to unity which we have sketched in Figure 2.

It should be noted that the frequency of exchange between the wells increases with the asymmetry of the potential. From eq 5 it follows that this frequency is given by

$$h\nu = 2\delta\,(1 + \rho^2)^{1/2} \qquad \nu/\nu_0 = (1 + \rho^2)^{1/2} \qquad (15)$$

In Figure 3 we represent the frequency ν as a function of the asymmetry parameter ρ.

It is worth noting that our eq 15 predicts an increase in the tunnelling frequency with increasing ρ. This is reasonable because the effect of the perturbation is always an increased separation of the two lowest energy levels and consequently the effect of the perturbation should cause an increase of the exchange frequency. We used eq 14 to describe the various systems that we studied previously[2-5,9] and we present the results in Table I. For methyloxonium ion and α-methyl-β-hydroxyacrolein the probability of finding the proton in well B is decreased by 3 and 2 orders of magnitude while in the case of 2-methylnaphthazarin tunnelling is completely eliminated. These results are consistent with the interpretation of current experimental data and with our previously published theoretical calculations. The result for 9-hydroxyphenalen-1-one is consistent with the currently available experimental evidence; it is identical with that calculated from the eigenstates of the asymmetric double-minimum potential by the variational method with a large basis set,[9] where the probability of tunnelling is obtained by numerical integration of the wave function in well B at time $t = \pi/2\omega$.

Intermolecular Pyrene Excimer Formation in Zeolites. Decay Parameters and Ground-State Association

Steven L. Suib* and Athanasios Kostapapas

Contribution from the Department of Chemistry and Institute of Materials Science, University of Connecticut, Storrs, Connecticut 06268. *Received May 25, 1984*

Abstract: Pyrene has been introduced into various zeolites in order to observe whether monomer or excimer formation dominates. Evidence has been found for ground-state association of pyrene, deposition of pyrene microcrystallites on external zeolite surfaces, and monomers and excimers inside the supercages of large-pore zeolites. The preparation of the materials controls what types of species will exist. Excimers in the supercages only exist if the zeolite has been dehydrated first. Solvents of varying polarity affect the luminescence in the monomer region. Quenching studies with Cs^+ ions and halonaphthalenes indicate that ground-state associated species can be dissociated. Luminescence lifetime, X-ray powder diffraction, and Fourier transform infrared experiments lend support to assignments of excimers, monomers, and ground-state-associated species and whether these are in internal or external sites.

The photochemical and photophysical behavior of fluorescent probes on solid surfaces has been sparsely studied. In recent years progress in this area has been made due to careful studies of well-defined supports, simple fluorescent probes, and molecular interactions. Pyrene has been used in several of these studies because the quantum yield of emission is high, the molecular

0002-7863/84/1506-7705$01.50/0

environment to be probed is normally not disturbed, excimers can form, and fluorescence decay measurements can be made over a reasonable time scale.

Surface photochemical reactions involving pyrene have dealt with translational motion over silica gel,[1-9] multisite adsorption on TiO_2 semiconducting powders,[10] quenching studies on clay colloids,[11] and photophysical studies on alumina,[12,13] CdS, and CaF_2.[14] None of these supports have regular three-dimensional pores that do not change when molecules are adsorbed.

For several years we have been studying the photochemical and photophysical behavior of inorganic[15,16] and organic[16,17] molecules in zeolite molecular sieve environments. It is the purpose of this paper to present measurements of the behavior of pyrene molecules both on the surface and in the pores of various zeolites. Luminescence and related spectroscopic measurements support the belief that pyrene monomers, excimers, and ground-state-associated species exist to varying extents in the zeolites, depending on the method of preparation.

Experimental Section

Materials. Zeolites X (Lot No. 08077), A (Lot No. 061576), and Y (Lot No. 042578, SK-40) were obtained in their sodium forms from Alfa Ventron Corp., Danvers, MA. Their surface areas were 750, 750, and 900 m^2/g, before exchange, respectively.

Cesium chloride (Lot No. 111781, 99.9% pure) was also obtained from the same vendor and was used without further purification.

Pyrene (Lot No. 102087, mp 155–156 °C) was purchased from Aldrich Chemical Comp., Milwaukee, WI. It was further purified by recrystallization twice from absolute ethanol prior to use.

The compound 2-bromonaphthalene (mp 59 °C) was obtained from Eastman Organic Chemicals, Rochester, NY. 2-Chloronaphthalene (Lot No. 1-4534, mp 60 °C) was obtained from J. T. Baker Chemical Co., Phillipsburg, NJ. Both of the substituted naphthalenes were purified by recrystallization from ethanol.

All solvents used were purchased from J. T. Baker Chemical Comp. and were of spectral grade. The solvents and all solutions used in the experiments were degassed by bubbling nitrogen gas through them, with stirring, for 1 h prior to use. This was done to prevent quenching by oxygen.

Zeolite Preparation. Both hydrated and dehydrated zeolites were used in the experiments. In the hydrated case the zeolites were used as received from the vendor. Dehydrated zeolites were prepared as follows. Five grams of the zeolite were placed on a vacuum line and were degassed without heating for 3 h at 5×10^{-4} torr. Heating of the zeolite started thereafter with a heating rate of 50 °C per h to a final temperature of 350 °C. The zeolite was left at this temperature overnight to further dehydrate.

The dehydrated zeolite was worked up the next morning in a glovebag which was flushed and evacuated three times with dry nitrogen. The dehydrated zeolite was placed in a vial, sealed with parafilm, and placed in an inert atmosphere glovebox until further use.

Rotovaped Samples. Both rotovaped and stirred samples of pyrene and zeolites were prepared for the experiments. For the rotovaped hydrated samples a measured aliquot of a degassed pyrene in ethanol solution (0.001 M) and 2.0 g of the zeolite were placed in a 500-mL round-bottom flask. The flask was swirled briefly and placed on a Büchi Model R110 rotary evaporator and rotated for 15 min to mix the suspension. After mixing the solvent was slowly driven off by heating the flask with a heat bath kept at 45 °C and by pulling vacuum with an aspirator. Samples were then collected in a vial after scraping them from the walls of the flask.

The samples were degassed at room temperature by placing 0.2 g of the sample in 3-mm i.d. quartz tubes and pumping for 2 h on a vacuum line at 1×10^{-4} torr. The quartz tubes were sealed under vacuum, and these samples were used for steady-state luminescence and lifetime measurements.

Stirred Samples. The stirred hydrated samples were prepared by placing 50 mL of a degassed pyrene in ethanol solution (0.025 M) and 2.0 g of the zeolite in a 250-mL round-bottom flask. The flask was stoppered and sealed with Teflon sleeves and Parafilm. The suspension was stirred for 24 h with a Teflon magnetic stirrer bar. After the mixture was stirred, the zeolites were collected on a 60-mL medium-size glass sintered funnel and washed with three 10-mL portions of absolute degassed ethanol.

Another set of samples were prepared under the same conditions but were not washed in order to see any differences in the steady-state luminescence, lifetime, and FT-IR measurements.

Dehydrated samples of pyrene on zeolites were prepared both ways, rotovaped, and stirred, with two minor modifications. First, all manipulations of the dehydrated zeolites, addition of solutions, and workup of the samples were done in a glovebag which was flushed three times with dry nitrogen. Second, in the case of the rotovaped samples, the Büchi rotovapor was flushed with dry nitrogen gas while the sample was being rotated. Slow evaporation of the solvent was then done and the sample was worked up in the glovebag where it was also placed in a quartz tube and degassed as mentioned above.

Quenching Experiments. Samples with 2-chloronaphthalene, 2-bromonaphthalene, and cesium chloride used as coadsorbents were prepared as mentioned above with use of 1.0-mg/mL solutions of the coadsorbents in absolute ethanol. The solution of the coadsorbent was added to the pyrene solution prior to addition of the zeolite.

Luminescence Measurements. Luminescence spectra were recorded on a double Czerny-Turner scanning monochromator, Model 1902, Spex Fluorolog spectrophotometer. Freshly made Rhodamine B solutions served as the reference detector which automatically corrected for changes in the excitation radiation. Both excitation and emission spectra were recorded with use of the front face mode of the instrument and a 2.50-mm-slit band-pass.

Lifetime measurements were made with a standard PRA Model 3000 system using the single photon counting technique. A hydrogen lamp firing at 30,000 pulses per second served as the excitation source. The excitation wavelength, 340 nm, was selected by the use of a 340-nm interference filter obtained from Corion Corp., Holliston, MA, which was placed between the sample and the excitation source.

Emission was monitored at right angles to the sample and luminescence lifetime data were collected at 474 nm (excimer) and 394 nm (monomer) by the use of a UV–vis monochromator obtained from PRA, London, Ontario. The monochromator was placed between the sample and the photomultiplier tube.

A Tracor Northern (Model TN-7200) multichannel analyzer and a PDP-1103 computer were used for data collection, storage, and manipulation. Deconvolution of the luminescence decay curves and statistical analyses were done with software provied by PRA Corp. of London, Ontario, Canada.

Infrared Experiments. Fourier transform infrared experiments were done on a Nicolet 60-SX FT-IR system using a diffuse reflectance attachment. Samples were mixed in a KBr matrix using a Wig-L-Bug and data were collected and automatically corrected for matrix and background effects by the use of a Nicolet 1180 computer interfaced to the FT-IR system.

X-ray Powder Diffraction. X-ray powder analyses of the hydrated and dehydrated zeolites were made with a DIANO-XRD 8000 X-ray powder diffractometer equipped with a Philips electronic source. Solid samples were mounted on glass slides that were lightly coated with vaseline. Samples were scanned, using Copper Kα radiation, at 2° 2θ/min.

(1) Bauer, R. K.; Borenstein, R.; de Mayo, P.; Okada, K.; Rafalska, M.; Ware, W. R.; Wu, K. C. *J. Am. Chem. Soc.* **1982**, *104*, 4635–4644.
(2) Hara, K.; de Mayo, P.; Ware, W. R.; Weedon, A. C.; Wong, G. S. K.; Wu, K. C. *Chem. Phys. Lett.* **1980**, *69*, 105–108.
(3) de Mayo, P.; Okada, K.; Rafalska, M.; Weedon, A. C.; Wong, G. S. K. *J. Chem. Soc., Chem. Commun.* **1981**, 820–821.
(4) de Mayo., P.; Nakamura, A.; Tsang, P. W. K.; Wong, S. K. *J. Am. Chem. Soc.* **1982**, *104*, 6824–6825.
(5) Johnston, L. J.; de Mayo, P.; Wong, S. K. *J. Chem. Soc., Chem. Commun.* **1982**, 1106–1108.
(6) Farwaha, R.; de Mayo, P.; Toong, Y. C. *J. Chem. Soc., Chem. Commun.* **1983**, 739–740.
(7) Bauer, R. K.; de Mayo, P.; Okada, K.; Ware, W. R.; Wu, K. C. *J. Phys. Chem.* **1983**, *87*, 460–466.
(8) Lochmüller, C. H.; Colburn, A. S.; Hunnicutt, M. L.; Harris, J. M. *Anal. Chem.* **1983**, *55*, 1344–1348.
(9) Francis, C.; Lin, J.; Singer, L. A. *Chem. Phys. Lett.* **1983**, *94*, 162–167.
(10) Chandrasekaran, K.; Thomas, J. K. *J. Am. Chem. Soc.* **1983**, *105*, 6383–6389.
(11) Della Guardia, R. A.; Thomas, J. K. *J. Phys. Chem.* **1983**, *87*, 3550–3557.
(12) Beck, G.; Thomas, J. K. *Chem. Phys. Lett.* **1983**, *94*, 553–557.
(13) Barber, R. A.; de Mayo, P.; Okada, K. *J. Chem. Soc., Chem. Commun.* **1982**, 1073–1074.
(14) Bauer, R. K.; de Mayo, P.; Ware, W. R.; Wu, K. C. *J. Phys. Chem.* **1982**, *86*, 3781–3789.
(15) Suib, S. L.; Bordeianu, O. G.; McMahon, K. C.; Psaras, D. In "Organic Reactions in Organized Media"; Holt, S. L., Ed.; American Chemical Society: Washington, 1982; ACS Symp. Ser. No. 177, pp 225–238.
(16) Suib, S. L.; Kostapapas, A.; Psaras, D. *J. Am. Chem. Soc.* **1984**, *106*, 1614–1620.
(17) Suib, S. L.; Kostapapas, A. Abstracts of the North East Regional ACS Meeting, Hartford, CT, 1983.

Table I. Luminescence Emission Bands of Pyrene-Containing Zeolites

zeolite	sample	condition[a]	[pyrene][b]	λ_{exc}[c]	I_e/I_m	I_{394}/I_{374}
NaX	1	H, R	8.98	337	2.32	1.65
				350	12.2	*d*
	2	D, R	8.98	337	0.25	1.36
				342	0.08	1.30
				349	0.09	1.40
	3	H, S	126.4	337	3.19	1.20
				343	7.24	1.13
	4	D, S	126.4	337	0.06	1.17
NaY	5	H, R	8.98	337	0.55	1.61
				347	1.55	1.85
	6	D, R	8.98	337	1.31	1.32
				352	5.09	2.88
	7	H, S	126.4	337	0.28	1.51
	8	D, S	126.4	337	0.38	1.30
NaA	9	H, R	8.98	337	5.75	3.33
	10	D, R	8.98	337	5.88	2.43
	11	H, S	126.4	337	7.55	1.83
	12	D, S	126.4	337	6.17	2.09

[a] H, hydrated; D, dehydrated; R, rotary evaporated; S, stirred. [b] mg of pyrene/g of zeolite. [c] In nm. [d] Excitation intensity observed only at 394 nm.

Table II. Luminescence Excitation Bands of Pyrene-Containing Zeolites

zeolite	sample no.	excitation monitored: 394 nm[a]	excitation monitored: at 474 nm[a]
NaX	1	322. 337, 372	326, 349, 372
	2	326, 342, 372	328, 349, 372
	3	310, 322, 337, 373	312, 325, 338, 375
	4	327, 343, 372 (sh)	327, 343, 372 (sh)
NaY	5	320, 337	329, 347, 372
	6	325, 340, 372	330 (sh), 346, 372 (sh)
	7	321, 335, 372 (sh)	323, 337, 372 (sh)
	8	325, 341, 372 (sh)	327, 344, 372 (sh)
NaA	9	332, 370	370
	10	322, 342, 372	325 (sh), 352 (sh), 371
	11	322, 337, 372	325, 348, 365
	12	322, 335, 372 (sh)	325, 340, 365

[a] In nm, sh = shoulder.

Further details of this research can be found elsewhere.[17]

Results

I. Luminescence Emission and Excitation. The luminescence emission and excitation behavior of pyrene (8.98 mg) per 1 g of zeolite for rotary evaporated, stirred, hydrated, and dehydrated materials are given in Table I. The zeolites that were studied include NaA, NaY, and NaX. The pyrene excimer and monomer regions were both monitored. An excimer excitation wavelength of about 350 nm, depending on the sample, and a monomer excitation of 337 nm were used throughout this study. The ratio of excimer emission intensity to monomer emission intensity (I_e/I_m), at 474 nm and 394 nm, respectively, is reported as is the vibrational fine structure ratio at 394 and 374 nm.

The nature of the excitation spectra change was monitored with the emission wavelength set at 394 or 474 nm. Table II lists the excitation bands for these pyrene-containing zeolites observed at both wavelengths.

Excitation spectra for zeolite NaY in the hydrated and dehydrated forms prepared by rotary evaporation and stirred techniques are given in Figure 1 for comparison purposes. Small pore zeolite NaA has different excitation characteristics as shown in Figure 2.

The luminescence emission spectra of a series of dehydrated and rotary evaporated zeolite samples are given in Figure 3. Samples prepared by stirring have quite different photochemical properties, and emission spectra are given in Figure 4 for contrast.

Samples that were rotary evaporated have pyrene emission and excitation bands that vary when the concentration of pyrene is changed. A series of experiments with concentrations of pyrene

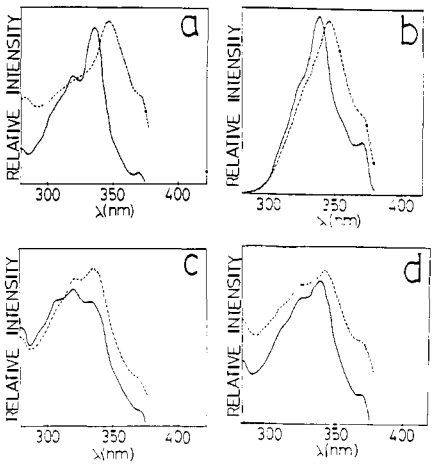

Figure 1. Luminescence excitation spectra of (a) hydrated rotary evaporated NaY, (b) dehydrated rotary evaporated NaY, (c) hydrated stirred NaY, and (d) dehydrated stirred NaY, (—) λ_{em} = 394 nm, (---) λ_{em} = 474 nm.

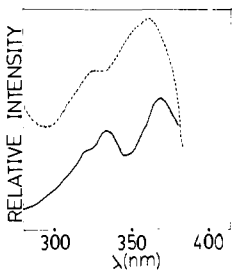

Figure 2. Luminescence excitation spectra of dehydrated stirred NaA zeolite, (—) λ_{em} = 394 nm, (---) λ_{em} = 474 nm.

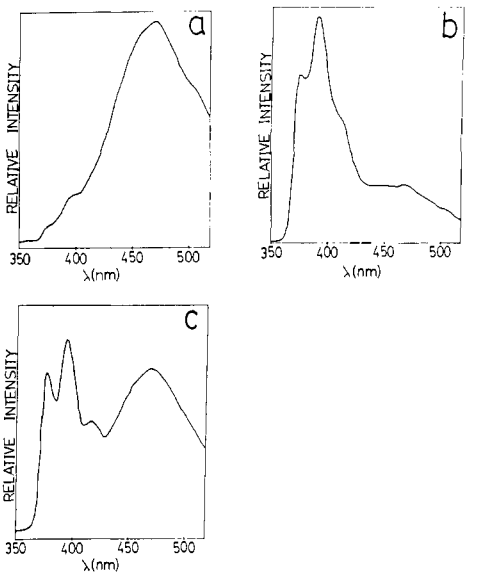

Figure 3. Luminescence emission spectra (λ_{exc} = 337 nm): (a) NaA, (b) NaX, (c) NaY. All samples were dehydrated and rotary evaporated.

varying from 0.05 mg of pyrene per g of zeolite to 20 mg of pyrene per g of zeolite are given in Table III. Hydrated rotary evaporated NaX is reported here. Hydrated rotary evaporated NaY gave similar results.

Emission characteristics for hydrated rotary evaporated NaX also change when the solvent is varied. A range of solvents having polar and nonpolar properties were used in the studies reported in Table IV. The emission of pyrene rotary evaporated from ethanol solution onto hydrated NaX zeolite can be quenched by various inorganic ions (Cs^+, Ag^+) as well as organic halonaphthalenes. The quenching characteristics of 2-chloronaphthalene are given in Table V. We note here that 2-

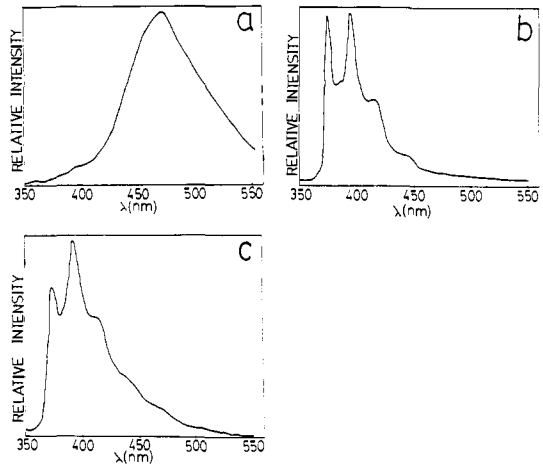

Figure 4. Luminescence emission spectra (λ_{exc} = 337 nm): (a) dehydrated stirred NaA, (b) hydrated stirred NaX, (c) dehydrated stirred NaY.

Table III. Excitation and Emission Characteristics for Pyrene on Hydrated Rotary Evaporated NaX Zeolite

T_{exc}[a]	[pyrene][b]	I_e/I_m	I_{394}/I_{374}	λ_{em}[a] 394	T_{em}[a] 474
337	0.05	0.43	1.20	322, 336	322, 336
322	0.05	0.45	1.32		
337	2.0	1.08	1.37	320, 336	325, 345, 372
345	2.0	3.13	1.50		
325	2.0	1.19	1.40		
320	2.0	1.00	1.42		
337	4.0	0.42	1.33	324, 338	326, 351, 373
351	4.0	2.74	1.49		
325	4.0	0.48	1.35		
337	6.0	0.70	1.49	325, 338	328, 351, 370
351	6.0	3.89	c		
337	8.0	1.08	1.60	322, 337	351, 370
351	8.0	4.32	c		
322	8.0	1.16	1.62		
337	10.0	0.45	1.52	322, 337	355, 375
355	10.0	3.33	c		
322	10.0	0.58	1.34		
337	20.0	0.83	1.66	323, 337	355, 375
355	20.0	4.84	c		
323	20.0	0.09	1.81		

[a] In nm. [b] mg of pyrene/g of zeolite. [c] No emission at 374 detected.

Table IV. Solvent Studies of Pyrene on Zeolite NaX

solvent	condition[a]	[pyrene][b]	λ_{exc}	I_e/I_m	I_{394}/I_{374}
ethanol	H, S	25 mg/50 mL	318	0.89	1.43
			334	0.89	1.43
			322	0.88	1.42
cyclohexane	H, S	25 mg/50 mL	320	0.24	1.20
			335	0.22	1.20
toluene	H, S	25 mg/50 mL	324	0.40	1.48
			335	0.22	1.48
			320	0.38	1.44
methanol	H, S	25 mg/50 mL	319	0.53	1.92
			332	0.50	1.80
			320	0.61	1.90
CH_3CN	H, S	25 mg/50 mL	320	0.57	1.69
			332	0.51	1.57
benzene	H, S	25 mg/50 mL	372	0.30	1.50
			334	0.24	1.38
			320	0.33	1.49
CCl_4	H, S	25 mg/50 mL	321	0.25	1.35
			335	0.21	1.43
			325	0.26	1.39

[a] See Table I, footnote *a*. [b] 2 g of zeolite used.

bromonaphthalene causes similar changes in the excitation and emission spectra.

II. Lifetime and Kinetic Experiments. A list of luminescence lifetime parameters of each of these species with preexponentials and a value of χ^2 is given in Table VI. Most of these systems turned out to have double exponential behavior although some had better fits to single exponential decays.

Table V. Quenching of Pyrene by 2-Chloronaphthalene Rotary Evaporated onto NaX

[Q]	λ_{exc}	I_e/I_m	I_{394}/I_{374}
	337 nm	0.069	1.16
		0.082	1.18
		0.090	1.18
2×10^{-5} mol/g	337 nm	0.246	1.22
		0.250	1.19
excimer abs	[348, 328]		
	348 nm	1.03	1.30
monomer abs	[321, 337]	1.12	1.28
4×10^{-5} mol/g	337 nm	1.32	1.22
		1.31	1.23
excimer abs	[345, 328]		
	345 nm	4.17	1.25
monomer abs	[337, 322]	4.05	1.18
	337 nm	1.26	1.22
6×10^{-5} mol/g	337 nm	4.42	1.20
excimer abs	[343, 327]		
	343 nm	8.47	1.18
monomer abs	[337, 322]		
8×10^{-5} mol/g	337	0.608	1.08
excimer abs	[328, 346]	1.40	1.34
	346 nm		
monomer abs	[322, 337]		
	337	0.407	1.27
10×10^{-5} mol/g	337 nm	0.643	1.20
		0.610	1.22
		0.626	1.18
excimer abs	[345, 327]		
	345 nm	1.72	1.28
monomer abs	[337, 322]		
	337 nm	0.586	1.22

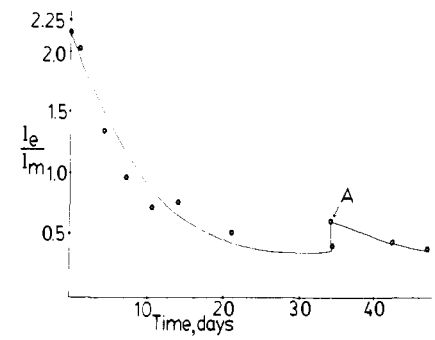

Figure 5. Ratio of excimer emission intensity to monomer emission intensity (I_e/I_m) vs. time. λ_{ex} = 337 nm, for hydrated rotary evaporated NaX.

The excimer to monomer emission intensity changes with time. A plot of (I_e/I_m) for a rotovaped hydrated NaX sample containing 2.02 mg of pyrene per g of zeolite is given in Figure 5. At point A, the sealed degassed quartz vial containing the pyrene zeolite sample was shaken. Similar behavior is noticed for all rotary evaporated samples. Dehydrated stirred X and Y zeolites do not show a large decrease in (I_e/I_m) with time.

Supporting Characterization Experiments. X-ray powder diffraction data for all of these samples and for recrystallized pyrene indicate that very intense peaks for pyrene occur at 22.6° 2θ which corresponds to a d spacing of 3.9 Å. A series of medium intensity bands for pyrene occur at 17.5° 2θ, 19.6° 2θ, 20.7° 2θ, and 22.0° 2θ. At least some of these bands were observed for the following samples: NaA, hydrated, stirred; NaY, hydrated, stirred; NaX, dehydrated, rotary evaporated; NaY, hydrated, rotary evaporated; NaX, hydrated, stirred; NaA, dehydrated, stirred; NaA, hydrated, rotary evaporated; NaA, hydrated, rotary evaporated; NaX, hydrated, rotary evaporated; NaY, dehydrated, rotary evaporated; NaA, dehydrated rotary evaporated; NaX, hydrated, stirred. The strongest matches of the zeolite samples with the recrystallized pyrene were for the zeolite A samples.

Table VI. Luminescence Lifetimes of Pyrene-Containing Zeolites

	emission monitored at 474 nm					emission monitored at 394 nm				
sample	A_1	A_2	τ_1	τ_2	χ^2	A_1	A_2	τ_1	τ_2	χ^2
NaX, H, R	−0.15	0.34	17.7 (8.1%)	90.5 (91.9%)	1.1	0.08	0.29	10.6 (4.2%)	68.1 (95.8%)	1.4
NaX, D, R	*a*	*a*	*a*	*a*	*a*	0.38		140 (100%)		1.5
NaX, H, S	0.12	0.32	2.8 (2.1%)	50.6 (97.9%)	1.4	*a*	*a*	*a*	*a*	*a*
NaX, D, S	*a*	*a*	*a*	*a*	*a*	0.02	0.31	12.5 (0.6%)	133 (99.4%)	2.7
NaY, H, R	−0.08	0.43	3.9 (1.3%)	53.6 (98.7%)	1.4	0.11	0.16	8.9 (8.7%)	64.5 (91.3%)	1.8
NaY, D, R	−0.06	0.43	5.8 (1.5%)	54.3 (98.5%)	1.6	0.16	0.10	6.3 (18.2%)	44.6 (81.8%)	1.4
NaY, H, S	0.09	0.21	4.8 (3.3%)	61.7 (96.6%)	1.9	0.07	0.22	7.6 (2.7%)	81.9 (97.3%)	2.1
NaY, D, S	−0.03	0.43	4.9 (0.6%)	57 (99.4%)	1.5	0.09	0.23	8.8 (5.8%)	57.1 (94.2%)	
NaA, H, R	0.37		52.2 (100%)		1.3	0.06	0.10	4.4 (6.0%)	43.9 (94.0%)	1.2
NaA, D, R	0.41		50.8 (100%)		1.5	*a*	*a*	*a*	*a*	*a*
NaA, H, S	0.41		50.7 (100%)		1.6	*a*	*a*	*a*	*a*	*a*
NaA, D, S	0.28		56.4 (100%)		1.5	*a*	*a*	*a*	*a*	*a*

[a] Emission too weak to detect.

Table VII. Fourier Transform Infrared Data for Pyrene Zeolite Samples

sample	treatment, exptl conditions[b]	band, cm^{-1}	intensity
pyrene solid	recrystallized from ethanol	839.9	very strong
NaX	D, R	838.9	weak
NaX	H, R	838.7	weak
NaX	H, S	838.1	weak
NaA	D, S	838.8	weak
NaA	H, R	840.8	weak
NaA	D, R	838.3	weak
NaY	H, R	837.9	weak
pyrene in ethanol	0.025 M/L of solution	846.0	weak
NaX, NaY	D, S	*a*	

[a] Too weak to observe by FTIR. [b] See Table I, footnote *a*.

Fourier transform infrared data for all of the pyrene-containing zeolite samples are given Table VII. Diffuse reflectance detection was used in these experiments.

Discussion

The molecular dimensions of the pyrene molecule are 7.2 Å by 13.0 Å.[18] The entrance into the internal cavities, supercages, of large-pore zeolites NaY and NaX is 7.4 Å.[19] Space-filling molecules of these faujasitic zeolites and pyrene indicate that pyrene could fit into the supercages provided that water and cations make way for the organic. The highest concentration of pyrene reported in this study is 20 mg of pyrene per g of zeolite. Assuming a surface area of 300 m^2/g for NaY and NaX (Linde) there would be 1 molecule of pyrene in an area of 500 $Å^2$. Although the calculation is not exact, it shows that we are dealing with coverages of pyrene and the zeolite surfaces that are less than monolayer coverage for all samples reported here.

Luminescence Excitation and Emission Spectra. The general excitation and emission spectral features for the rotary evaporated and stirred samples are very different. Dehydration of the zeolite before introduction of the pyrene by the rotovap or stirred methods also influences the luminescence features. The I_{394}/I_{374} ratio according to Thomas[20] gives a good indication of the polarity of the microenvironment of pyrene in micelles. Similar trends should be observed for zeolites. The higher the I_{394}/I_{374} ratio the more nonpolar the environment. This vibronic fine structure ratio as given in Table I for NaA zeolite is significantly higher than that for the other zeolites. The excimer-to-monomer ratio for NaA also shown in Table I is also higher than that for other zeolites. The method of incorporation of pyrene into NaA does not significantly alter either of these ratios. The emission data for NaA indicate that significant amounts of pyrene excimers or ground-state-associated dimers (vide infra) form on this small-pore zeolite.

The excitation spectra for these pyrene-containing zeolites provide information regarding ground-state association. The four excitation spectra shown in Figure 1 have been collected with emission wavelengths of either 474 nm (excimer or association) or 394 nm (monomer). The dehydrated rotary evaporated NaY, hydrated stirred NaX, and hydrated rotary evaporated NaY zeolite samples all show shifts in excitation bands when the emission wavelength is changed from 394 to 474 nm. This effect has been observed on silica gel and has been attributed to the presence of some ground-state association (perhaps dimeric).[2] This shift in excitation band on changing the emission wavelength does not occur for dehydrated stirred NaY as observed in Figure 1. Dehydrated stirred NaX is the only zeolite sample studied that does not show this shift. Consequently, significant amounts of ground-state association do not occur when the zeolite is first dehydrated followed by pyrene introduction by slow exchange.

Excitation spectra for dehydrated stirred NaA as in Figure 2 show peaks at 365 and 372 nm for λ_{em} = 474 and 394 nm, respectively. These spectra indicate that substantial ground-state association occurs on NaA. Similar excitation spectra for other methods of preparation of pyrene on NaA were obtained.

Luminescence excitation bands for all 12 samples are given in Table II. NaX and NaY show similar luminescence emission and excitation spectra for similar preparations. The NaA samples are different than NaY and NaX and seem to remain about the same for all preparations.

The emission spectra of rotary evaporated samples show much more emission at longer wavelengths in the excimer/ground-state-associated band than for stirred samples. The emission

(18) Bower, H. J. M. "Tables of Interatomic Distances and Configurations in Molecules and Ions"; Burlington House: The Chemical Society, London, 1958; Special Publication II.

(19) Smith, J. V. In "Zeolite Chemistry and Catalysis"; Rabo, J. A., Ed.; American Chemical Society: Washington, 1976; ACS Monograph Series, Vol. 171, Chapter 1.

(20) Kalyanasurdaram, K.; Thomas, J. K. *J. Am. Chem. Soc.* **1977**, *99*, 2039–2044.

spectra of Figure 3 reveal a very strong excimer emission at 470 nm and a weak monomer emission. Dehydrated NaY shows more excimer than dehydrated NaX, but significant amounts in the excimer and ground-state-associated region (~474 nm) exist in both samples.

The emission spectra in Figure 4 provide complimentary information with respect to the samples shown in Figure 3. The dehydrated NaA containing pyrene introduced by stirring still has very little monomer emission. The hydrated NaX sample with pyrene prepared by stirring has an odd monomer emission and some emission at longer wavelengths. The dehydrated stirred NaY sample has some excimer/ground-state-association contribution, but the major emission is due to monomer. The dehydrated stirred NaX zeolite has an emission spectrum (not shown) virtually identical with that of the dehydrated stirred NaY zeolite sample shown in Figure 4.

The emission and excitation spectra for the samples discussed above suggest that the pyrene microenvironment on NaA is very much different than that of either NaX and NaY. Close examination of the data for NaA indicate similarities in excitation and emission spectra for microcrystalline particles of pyrene on the surface. Room-temperature and low-temperature spectra of NaA are strikingly similar to other reports of microcrystalline pyrene.[21,22]

The emission and excitation spectra of hydrated NaX with pyrene prepared by the rotary evaporation method change with varying amounts of pyrene. As more and more pyrene is added as shown in Table III, the I_e/I_m ratio increases. The I_{394}/I_{374} ratio also increases, indicating that the environment on the surface is becoming more nonpolar in character. A corresponding shift in the excitation bands also occurs. For instance, at a 0.05 mg concentration of pyrene the excitation wavelengths are located at 322 and 336 nm. At a concentration of 4.0 mg these maxima shift to 326 and 351 nm and a new band at 373 nm appears. At very high pyrene concentration, 20 mg, the low-wavelength band disappears and the other 2 bands red shift to 355 and 375 nm. More ground-state association is occurring as more and more pyrene associates on the outer surface of these rotary-evaporated zeolites.

The solvent used to prepare the rotary-evaporated materials also affects the luminescence properties of the samples. The order of increasing polarity of solvents used is cyclohexane ~ CCl_4 < toluene < benzene < ethanol < methanol < CH_3CN. Examination of the I_{394}/I_{374} ratio from Table IV indicates a fairly uniform ratio which does not seem to indicate any noticeable trend. This suggests that the polarity of the external surface sites is controlled by zeolitic properties and that the solvent does not noticeably affect where the pyrene particles deposit. This belief is reinforced by the similarity in the excimer to monomer intensity ratio for all different solvents.

The quenching effects of halonaphthalenes shown in Table V yield an increase in I_e/I_m up to a concentration of 8×10^{-5} mol of 2-chloronaphthalene per g of zeolite when the I_e/I_m ratio then begins to decrease. It has earlier been suggested that ground-state-associated pyrene species on silica are broken up by addition of halonaphthalene due to occupation of surface sites by the quencher.[1] Similar processes are occurring on the zeolite surfaces that contain pyrene prepared by the rotary evaporation method.

Luminescence Lifetime and Kinetic Experiments. Lifetime data for these systems as summarized in Table VI provide information regarding ground-state association.[1,8] True excimer kinetics should yield A_1 and A_2 values for double exponentials that are equal in magnitude but opposite in sign. Others[1,2,7,14,24,25] have suggested that the divergence of the A_1/A_2 ratio from a value of −1 gives an indication of the amount of ground-state association. The lifetime data for all samples show that decay solely due to excimer is never achieved. For example, the dehydrated stirred NaY sample does show opposite signs for A_1 and A_2 but of different magnitude. The NaA decay is dominated by excimer and ground-state association decay with only very weak emission in the monomer region.

Supporting Spectroscopic Experiments. X-ray powder diffraction experiments indicate that all samples besides the dehydrated stirred NaX and NaY show some microcrystalline pyrene particles on their surfaces as evidenced by similar diffraction peaks.

The Fourier transform infrared data of Table VII show that a band between 838 and 841 cm^{-1} appears in all samples except the dehydrated stirred NaX and NaY samples. Pyrene as a solid shows a band at 839.9 cm^{-1}, but pyrene in solution shows a very weak band at 846 cm^{-1} even at farily high concentrations. The amount of pyrene in the dehydrated stirred NaX and NaY samples is of the same order as all other samples of Table VII. This suggests that the dehydrated stirred NaY and NaX samples are different than the other materials, perhaps having pyrene in a solution-like environment[16] in the supercages of these large-pore zeolites. The luminescence emission and excitation data and the X-ray powder diffraction data reported above support this belief.

Overview

The results of experiments described above suggest that zeolite samples containing pyrene deposited with the rotary evaporation method have monomeric and ground-state-associated species on external surfaces of the zeolite. Solvent does not affect the distribution of pyrene. The ground-state-associated species[1,2,8] can be monitored with luminescence excitation and lifetime experiments and can be dissociated with various quenchers.

Samples prepared by the stirred method give results that indicate that hydrated zeolites do not allow pyrene to enter the supercages. On dehydration of large-pore zeolites pyrene does enter the supercages as evidenced by emission, excitation, lifetime, and infrared results. During preparation of this manusript we became aware of similar study regarding pyrenealdehyde in zeolite X.[23] Our results and the steric requirements of the aldehyde suggest that it would be more difficult and perhaps impossible for the pyrenealdehyde to enter the supercages of a hydrated NaY zeolite.

The kinetic behavior of excimer and monomer species in these zeolites may be important in studies of diffusion of molecules in zeolite pores. Thermodynamic parameters can be derived from variable-temperature luminescence studies of these zeolites.[26] This study shows the use of organic luminescent molecules as probes of external and internal zeolite surfaces.

Acknowledgment. We thank D. Psaras for help in collection of the luminescence lifetime data and G. Lavigne for help with FTIR measurements. The generous support of the National Science Foundation under Grant NSF-CHE 820441F is gratefully acknowledged.

(21) Ferguson, J. *J. Chem. Phys.* **1958**, *28*, 765–768.
(22) Takahashi, Y.; Kitamura, T.; Uchida, K. *J. Lum.* **1982**, *27*, 449–453.
(23) Baretz, B. H.; Turro, N. J. *J. Photochem.* **1984**, *24*, 201–205.
(24) MacCallum, J. R. *Eur. Polym. J.* **1981**, *17*, 797–799.
(25) Takahashi, Y.; Kitamura, T.; Uchida, K.; Tomura, M. *J. Lum.* **1981**, *22*, 267–271.
(26) Suib, S. L.; Kostapapas, A., unpublished results.